Thermochimica Acta 514 (2011) 58–66

Contents lists available at ScienceDirect

Thermochimica Acta

journal homepage: www.elsevier.com/locate/tca

Thermal degradation kinetics and isoconversional analysis of biodegradable poly(3-hydroxybutyrate)/organomodified montmorillonite nanocomposites

Dimitris S. Achilias[a,*], Elpiniki Panayotidou[a,b], Ioannis Zuburtikudis[b]

[a] Laboratory of Organic Chemical Technology, Department of Chemistry, Aristotle University of Thessaloniki, 54124 Thessaloniki, Greece
[b] Department of Industrial Design Engineering, TEI of Western Macedonia, 50100 Kozani, Greece

ARTICLE INFO

Article history:
Received 14 September 2010
Received in revised form 1 December 2010
Accepted 9 December 2010
Available online 21 December 2010

Keywords:
Degradation kinetics
Isoconversional analysis
Poly(3-hydroxybutyrate)
Nanocomposites
Biodegradable polymers

ABSTRACT

Poly(3-hydroxybutyrate) (PHB)/organically modified clay nanocomposites were prepared by the melt mixing method and were characterized using wide-angle X-ray diffraction. Their thermal degradation kinetics was investigated using thermogravimetric analysis at various heating rates. Further kinetic analysis was performed using isoconversional methods and the invariant kinetic parameters method was used to estimate the so-called 'true' kinetic parameters, i.e. the pre-exponential factor, A and the activation energy, E, as well as the reaction model. It was found that intercalated structures are formed and the thermal stability of the material is improved by the addition of the nano-filler. From the isoconversional analysis, it was found that the activation energy does not vary significantly with the degree of degradation denoting degradation in one step with similar values for pure PHB and for all nanocomposites. Using the invariant kinetic parameters method, it was found that the model that best describes the experimental data was that of Sestak–Berggren's with $f(a)=\alpha^n(1-\alpha)^m$, where the value of n is always larger than m and is increasing with the amount of the nano-filler. The value of the 'true' activation energy was found to be about 100 kJ mol^{-1} for all nanocomposites and the pre-exponential factor for PHB was estimated equal to 5.35×10^9 min^{-1}. Finally, the values of the kinetic rate constant k were found to decrease with the amount of the nano-filler up to 3 wt%, while for amounts larger than 3 wt% k increased reaching a value greater than that of pure PHB for the 10 wt% nanocomposites.

1. Introduction

Recently, biodegradable and biocompatible polymers have received significant attention, because they are environmental-friendly and are extensively used in the biomedical applications. Since biopolymers are obtained from renewable resources, they represent an interesting alternative route to common non-degradable polymers for short-life range applications (packaging, agriculture, etc.). Poly(3-hydroxybutyrate) (PHB) is such a fully biodegradable, thermoplastic aliphatic polyester, produced by a wide variety of bacteria from cheap renewable raw materials, which has some physical and mechanical properties comparable to those of isotactic polypropylene [1]. Because of these properties, PHB has attracted a lot of attention by the research community. However, it has some drawbacks such as stiffness, brittleness, and most of all very low thermal stability at processing temperatures slightly higher than its melting point that prevent its commercial use to a bigger extent applications. The thermal instability of PHB in the melt prevents it from substituting the non-biodegradable polymeric materials in commercial products [2]. That is why improving the thermal stability of PHB is very important. There are several approaches to overcome these drawbacks of PHB: (a) biosynthesize series of copolymers containing hydroxyalcanoate units other than 3-hydroxybutyrate units, (b) prepare miscible blends of PHB with another bio-degradable polymer with suitable properties or plasticizer, and (c) synthesize block copolymers based on PHB. As an alternative to these conventional methods, the preparation of PHB nanocomposites is investigated here.

Polymer nanocomposites are commonly defined as the combination of a polymeric matrix and fillers that have at least one dimension (i.e. length, width or thickness) in the nanoscale. Nano-biocomposites are very promising materials, since they show improved properties with preservation of the material biodegradability, without eco-toxicity. Such materials are mainly destined to biomedical applications and different short-term applications, e.g., packaging, agriculture or hygiene devices. They, thus, represent a strong and emerging answer for improved and eco-friendly materials [3]. It has been shown that, only with a few percent of nanofiller (usually from 1 to 5 wt%), the polymer nanocomposites often exhibit greatly improved thermal, mechanical and barrier properties compared to pristine polymer. Commercially, the most important type of polymer nanocomposites are those produced

* Corresponding author. Tel.: +30 2310 997822; fax: +30 2310 997769.
E-mail address: axilias@chem.auth.gr (D.S. Achilias).

0040-6031/$ – see front matter © 2010 Elsevier B.V. All rights reserved.
doi:10.1016/j.tca.2010.12.003

using layered clay minerals (2:1 phyllosilicates), especially montmorillonite, that are naturally abundant, environmentally friendly and economic. Montmorillonite is usually chemically modified by a cation-exchange method, by which its sodium counterions are exchanged with adequate organic, usually alkyl ammonium, cations, in order to match its compatibility with polymer matrix, which is the key to successful preparation of polymer nanocomposites.

Thermogravimetric analysis (TGA) is a common experimental method used to study the overall or macroscopic kinetics of polymer degradation. The determination of the parameters of the thermal decomposition process provides more specific information regarding internal structures of polymeric materials [4,5]. However, apart from a simple TGA scan, further computational kinetic analysis is needed to probe the degradation mechanism, as well as to predict the thermal stability of polymers. Among others, isoconversional methods have been conceived by many researchers and widely used in the thermal degradation kinetic studies [6].

Although the thermal degradation kinetics of PHB and copolymers based on PHB has been studied in the literature [7–14] only two articles have been published so far on the non-isothermal degradation of PHB nanocomposites [15,16], in combination with other two for isothermal degradation [17,18]. In the work of Erceg et al. [15,16], nanocomposites of PHB with commercial organomodified MMT under the trade names Cloisite 25A and 30B prepared by the solution-intercalation method, were employed.

In the present work, various loadings of montmorillonite organically modified by octadecylamine (C_{18}MMT) were dispersed in PHB using a micro-extruder/compounder. The aim was to produce hybrid material with improved thermal properties over the pristine PHB. Constant nitrogen flow during nanocomposite preparation prevented thermal decomposition of the matrix. The nanocomposites were characterized by X-ray diffraction (XRD). Then, the non-isothermal degradation of pure PHB and PHB/C_{18}MMT nanocomposites, as well as the influence of C_{18}MMT on the thermal stability of PHB, was investigated and a detailed kinetic analysis of the process was performed using model-based and model-free methods. In particular, isoconversional methods were employed for the determination of the variation of the activation energy with respect to the degree of degradation and the invariant kinetic parameters were estimated together with the so-called 'true' activation energy and pre-exponential factor. Finally, a kinetic model was proposed and its parameters were evaluated.

2. Experimental

2.1. Materials

Poly(3-hydroxybutyrate) (PHB) was supplied by Sigma–Aldrich Chemical Co. and used as received. Sodium montmorillonite (NaMMT) with a cation exchange capacity (CEC) = 92.6 mequiv./100 g was obtained from Southern Clay Products (Texas, USA) and was dried in a vacuum oven at 80 °C for 24 h before use. Octadecylamine and concentrated HCl were purchased from Sigma–Aldrich and used without any further purification. Organically modified montmorillonite C_{18}MMT was prepared by an ion exchange reaction between NaMMT and octadecylammonium salt [19]. The relevant quantity of octadecylamine weighed out and through the cation-exchange proceeding received the final product. It was stored in a desiccator until its use.

2.2. Preparation of specimens

.

The nanocomposites were prepared by melt mixing of PHB with different amounts of C_{18}MMT in a co-rotating twin screw micro-extruder (MiniLab® by Thermo-Haake). The melt mixing was carried out at 175 °C for 3 min and 130 rpm. Constant nitrogen flow was used during nanocomposite preparation in order to prevent thermal decomposition of the polymer matrix. Nanocomposites containing 1, 3, 5 and 10 wt.% of C_{18}MMT were prepared.

2.3. Measurements

Wide angle X-ray diffraction (WAXD): XRD patterns were obtained using an X-ray diffractometer (3003 TT, Rich. Seifert) equipped with Cu Kα generator (λ = 0.1540 nm). Scans were taken in the range of the diffraction angle 2θ = 1–10°.

2.4. Thermogravimetric analysis (TGA)

TGA was performed on a Pyris 1 TGA (Perkin Elmer) thermal analyzer. Samples of about 10 mg were used. They were heated from ambient temperature to 400 °C under a 20 ml/min nitrogen flow. TGA measurements of each sample were performed at different heating rates of 2.5, 5, 10 and 20 °C min^{-1} and sample mass versus temperature was continuously recorded.

3. Kinetic analysis of the TGA data

The kinetics of polymer degradation is usually described by the following single-step kinetic equation [6,20]:

$$\frac{d\alpha}{dt} \equiv \beta\frac{d\alpha}{dT} = k(T)f(\alpha) = A\exp\left(\frac{-E}{RT}\right)f(\alpha) \quad (1)$$

where α represents the extent of reaction, which can be determined from TGA runs as a fractional mass loss, β is the linear heating rate, t is time, $k(T)$ a temperature dependent rate constant usually expressed by an Arrhenius-type expression with A and E the pre-exponential factor and the activation energy, respectively and $f(\alpha)$ denotes the particular reaction model, which describes the dependence of the reaction rate on the extent of reaction.

In Eq. (1), the mutual dependence of the Arrhenius parameters A and E, which, in turn, are affected by the choice of the kinetic model function, $f(\alpha)$, recommends that at least one of the kinetic triplet $[A, E, f(\alpha)]$ elements should be computed independently from the others. In this work, in order to estimate the kinetic parameters of the non-isothermal degradation of pure PHB and its nanocomposites with different amounts of C_{18}MMT both isoconversional methods (such as the method of Friedman's, Flynn–Wall–Ozawa's and Kissinger–Akahira–Sunose's) and the invariant kinetic parameters (IKP) method were used.

3.1. Isoconversional methods

Isoconversional methods employ multiple temperature programs (e.g., different heating rates) in order to obtain data on varying rates at a constant extent of conversion. Thus, isoconversional methods allow complex (i.e. multi-step) processes to be detected via a variation of E_α with α [6].

Simple rearrangement of Eq. (1) leads to Eq. (2), which forms the foundation of the differential isoconversional method of Friedman's [21]

$$\ln\left(\frac{d\alpha}{dt}\right)_{\alpha,i} \equiv \ln\left(\beta_i\frac{d\alpha}{dT}\right)_\alpha = \ln[A_\alpha f(\alpha)] - \frac{E_\alpha}{RT_{\alpha,i}} \quad (2)$$

where the subscript α denotes value at a specific extent of reaction and the subscript i denotes different heating rates.

Then, for a specific extent of reaction, α, plotting $\ln(d\alpha/dt)$ versus $1/T$ obtained from α–T curves at several heating rates, should result in a straight line with a slope equal to the activation energy, E_α, at this conversion. Application of the Friedman method to the integral part (e.g., TGA data) requires numerical differentiation of the experimental α versus T curves. This is typically carried out by the software of the instrument used and in sometimes results in quite noisy rate data and thus, unstable activation energy values. This problem of numerical differentiation could be avoided by using integral isoconversional methods. For nonisothermal conditions, when the temperature is raised at a constant heating rate β, integration of Eq. (1) involves solving the temperature integral in Eq. (3):

$$g(\alpha) \equiv \int_0^\alpha \frac{d\alpha}{f(\alpha)} = \frac{A}{\beta}\int_{T_0}^{T_\alpha} \exp\left(\frac{-E}{RT}\right) dT = \frac{A}{\beta} I(E,T) \tag{3}$$

Since the integral $I(E,T)$ in Eq. (3) does not have an analytical solution it can be solved using either approximations or numerical integration. One of the simplest approximations by Doyle's [22] gives rise to the following Eq. (4), which is used in the popular isoconversional methods of Flynn and Wall's [23] and Ozawa's [24].

$$\ln(\beta_i) = \ln\frac{AE_\alpha}{Rg(\alpha)} - 5.331 - 1.052\frac{E_\alpha}{RT_{\alpha,i}} \tag{4}$$

According to this method, the activation energy is calculated at given values of conversion from a plot of $\ln(\beta_i)$ versus $1/T_i$. It is important that this method provides estimation of E_α without knowledge of the specific reaction function. The OFW method assumes that E_a is constant, thus a systematic error in the estimation of E_a should be expected, whenever E_a varies with a [6].

Use of another asymptotic approximation for the integral yielded the following equation, known as the Kissinger–Akahira–Sunose method (KAS).

$$\ln\left(\frac{\beta_i}{T_{\alpha,i}^2}\right) = \ln\frac{AR}{E_\alpha g(\alpha)} - \frac{E_\alpha}{RT_{\alpha,i}} \tag{5}$$

Evaluation of the activation energy is achieved from the plot of the left hand side of Eq. (5) versus $1/T_{\alpha,i}$ at constant degrees of conversion and heating rate.

Further increase in precision of the integral methods can be accomplished by using numerical integration, a method developed and extensively used by Vyazovkin [25,26].

3.2. Kissinger's method

Apart from the isoconversional methods described above, a method widely used in the literature to determine the activation energy of solid-state reactions is that of Kissinger's [27]. According to Kissinger's method the activation energy can be determined from a plot of the logarithm of the heating rate over the squared temperature at the maximum reaction rate, T_{max}, versus the inverse of T_{max} in constant heating rate experiments, from:

$$\ln\left(\frac{\beta_i}{T_{\max,i}^2}\right) = \text{Const.} - \frac{E}{RT_{\max,i}} \tag{6}$$

where T_{max} is the temperature corresponding to the inflection point of the thermo-degradation curve, which corresponds to the maximum reaction rate.

The activation energy can be calculated according to this method without a precise knowledge of the reaction mechanism. The applicability of the Kissinger equation in thermal analysis has been recently revisited [28].

3.3. Determination of the reaction mechanism

3.3.1. The master plot method [29–31]

According to this method, master plots can be drawn based on either the integral or the differential form of the kinetic equation describing degradation by using the concept of the generalized time, θ. From the integral kinetic equation the following equation can be obtained using a reference point at $\alpha = 0.5$

$$\frac{g(\alpha)}{g(0.5)} = \frac{\theta}{\theta_{0.5}} \tag{7}$$

During non-isothermal experiments at a linear heating rate, the right-hand side of Eq. (7) can be calculated by

$$\frac{\theta}{\theta_{0.5}} = \frac{p(x)}{p(x_{0.5})} \tag{8}$$

where for the function $p(x)$ the fourth rational approximation of Senum and Yang corrected by Flynn was used (Eq. (9)), which allows an accuracy of better than 10^{-5}% [29]:

$$p(x) = \frac{\exp(-x)}{x}\pi(x) \tag{9}$$

and

$$\pi(x) = \frac{x^3 + 18x^2 + 86x + 96}{x^4 + 20x^3 + 120x^2 + 240x + 120} \tag{10}$$

where $x = E/RT$.

3.3.2. The invariant kinetic parameters (IKP) method [32]

Furthermore, the 'true' kinetic model can be obtained using the invariant kinetic parameters (IKP) method. Accordingly, sets of $\ln A$ and E are obtained at different heating rates using the Coats and Redfern (CR) method [33]

$$\ln\frac{g(\alpha)}{T_{\alpha,i}^2} = \ln\frac{AR}{E_\alpha\beta_i} - \frac{E_\alpha}{RT_{\alpha,i}} \tag{11}$$

Algebraic expressions for $g(\alpha)$ for the most frequently used mechanisms appear in Table 1. For each theoretical kinetic model, $g(\alpha)$, and at each heating rate, β, from the slope and the intercept of plots $\ln[g(\alpha)/T^2]$ versus $1/T$, the parameters $\ln A$ and E can be evaluated.

If the compensation effect between $\ln A$ and E exists, then by plotting $\ln A$ versus E straight lines should be obtained for each heating rate, according to

$$\ln A = \alpha^* + b^* E \tag{12}$$

These lines should intersect in a point that corresponds to the 'true' values of E and $\ln A$ for the 'true' kinetic model, which were called by Lesnikovich and Levchik the invariant kinetic parameters, E_{inv} and A_{inv} [34]. Due to the fact that certain variations of the experimental conditions determine regions of intersection, the intersection is only approximate. Therefore, in order to eliminate the influence of experimental conditions on the determination of A_{inv} and E_{inv}, they are determined from the slope and intersect of the so-called supercorrelation relation:

$$\alpha^* = \ln A_{inv} - b^* E_{inv} \tag{13}$$

It should be noted here that the IKP method can be used only if E does not depend on α; a prerequisite that should be previously checked by isoconversional methods. Then, IKP method can be used for the numerical evaluation of the $f_{inv}(\alpha)$ by introducing values of the invariant kinetic parameters E_{inv} and A_{inv}.

Table 1
Expressions for $f(\alpha)$ and $g(\alpha)$ for the most frequently used mechanisms.

Mechanism	Symbol	$f(\alpha)$	$g(\alpha)$
Reaction order model	F_n	$(1-\alpha)^n$	$-\ln(1-\alpha)$, for $n=1$ $[1-(1-\alpha)^{1-n}]/(1-n)$, for $n \neq 1$
Phase boundary controlled reaction (area)	R_2	$(1-\alpha)^{1/2}$	$2[1-(1-\alpha)^{1/2}]$
Phase boundary controlled reaction (volume)	R_3	$(1-\alpha)^{2/3}$	$3[1-(1-\alpha)^{1/3}]$
Random nucleation and growth of nuclei (Avrami–Erofeev, JMA model)	A_m $(0.5 \leq m \leq 4)$	$m(1-\alpha)[-\ln(1-\alpha)]^{(1-1/m)}$	$[-\ln(1-\alpha)]^{1/m}$
1D diffusion	D_1	$1/(2\alpha)$	α^2
2D diffusion	D_2	$1/[-\ln(1-\alpha)]$	$(1-\alpha)\ln(1-\alpha)+\alpha$
3D diffusion	D_3	$(3(1-\alpha)^{2/3})/\{2[1-(1-\alpha)^{1/3}]\}$	$[1-(1-\alpha)^{1/3}]^2$
3D diffusion	D_4	$3/\{2[(1-\alpha)^{-1/3}-1]\}$	$(1-2\alpha/3)-(1-\alpha)^{2/3}$
Sestak–Berggren	SB (n,m)	$\alpha^n(1-\alpha)^m$	

4. Results and discussion

Polymer–clay nanocomposites could be characterized as intercalated, partially exfoliated or exfoliated. The particular form depends on the clay content, the chemical nature of the organic modifier and the synthetic method. In general, an exfoliated system is more feasible with lower clay content (about 1 wt%), while an intercalated structure is frequently observed for nanocomposites with higher clay content. XRD results for pure nano-filler C_{18}NMMT and all PHB/C_{18}NMMT nanocomposites appear in Fig. 1. It can be seen that the peak at 4.5° present in the NaMMT is shifted to lower 2θ values for the hybrid materials denoting an intercalated structure. No significant peak was found for PHB/1 wt% C_{18}NMMT suggesting exfoliated or partially exfoliated and intercalated structure. (TEM would give a definite answer to which of those possibilities is more likely to happen.)

Indicative thermal degradation curves of pure PHB and PHB/C_{18}MMT nanocomposites with different relative amounts of the organomodified MMT appear in Fig. 2. Similar curves were obtained at all different heating rates. It is seen that, as the amount of C_{18}MMT is increased from 1 to 5 wt%, the curves are shifted to higher temperatures indicating the production of a material with improved thermal stability. At the highest amount of 10 wt% C_{18}MMT, the degradation starts slightly later compared to that with 5 wt%, although it drops down with a higher rate. Moreover, the temperature at the maximum of the thermal decomposition, T_p, was found to increase with the amount of C_{18}MMT until 5 wt%, while, after that composition, it slightly decreases (Table 2). Similar results were observed for the conversion at T_p and for the temperature to achieve 50% conversion, $T_{1/2}$, seen in Table 2, at all heating rates investigated. The residual mass at 400 °C of pure PHB and of the nanocomposites with 1, 3, 5 and 10 wt% C_{18}MMT were around 1, 1.3, 2.6, 4 and 7.5 wt%, respectively.

4.1. Estimation of the effective activation energy

Initially, the activation energy was estimated using isoconversional methods. In this way, the complexity of the process could be established. This could be accomplished by plotting E versus α. FWO, KAS and the Friedman methods were employed. However, since the method of FWO provides almost the same results with the KAS [4] and is somehow inferior to KAS, all further results and discussion are based only on the latter method. For selected α values from 5% to 95% plots of $\ln(\beta/T^2)$ versus $1/T$, according to the KAS method, were constructed for PHB and all nanocomposites. From the slope of the straight lines thus obtained the values of E were calculated. In every case, the correlation coefficient was not less than 0.999. The obtained values are plotted as a function of α in Fig. 3 for pure PHB and all nanocomposites. Furthermore, E values were estimated using the differential method of Friedman. The differences between the integral and the differential results can be explained by their different intrinsic nature. The Friedman method is prone to be very sensitive to experimental data due to the magnification of the instrumental noise in the calculation of the derivatives. In this case, these data were noisy enough and we decided not to include them in the results. As it can be seen in Fig. 3, the variation of E with α is very small (i.e. less than 10 kJ/mol and only 3 kJ/mol in some samples) for all samples investigated and over almost the complete conversion range. Therefore, from a kinetic point of view, it could be assumed that the degradation of PHB and PHB nanocomposites

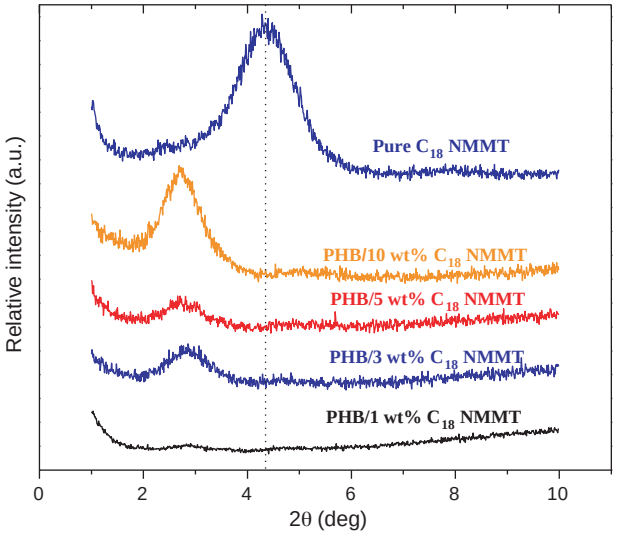

Fig. 1. XRD spectra of pure C_{18}NMMT and of PHB hybrid materials with different amounts of C_{18}NMMT prepared via melt mixing.

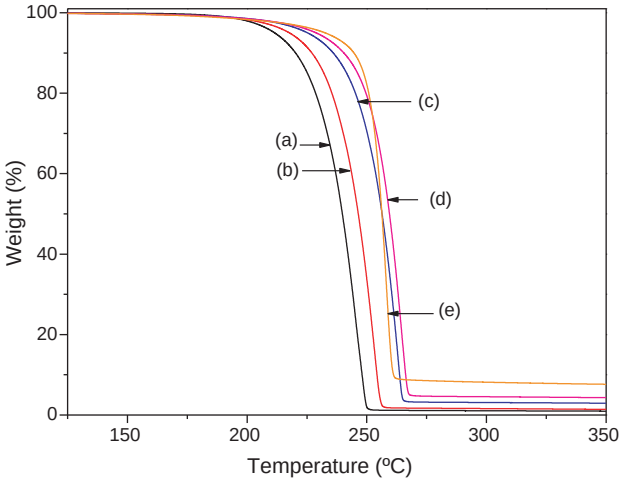

Fig. 2. Thermal degradation curves of PHB (a) and PHB nanocomposites with 1 wt% (b), 3 wt% (c), 5 wt% (d) and 10 wt% C_{18}MMT (e) after heating at 5 °C/min.

Table 2
Characteristic quantities obtained from the TG and DTG curves for all PHB-based nanocomposites studied at different heating rates. T_{on}: extrapolated onset temperature (T_{on}); T_p: temperature at the maximum of thermal decomposition; $T_{1/2}$: temperature at 50% conversion; α_p: conversion at T_p; RM: residual mass at 400 °C.

Sample	Heating rate (°C/min)	T_{on} (°C)	T_p (°C)	$T_{1/2}$ (°C)	α_p (%)	RM (%)
PHB	2.5	202.4	231.0	222.0	79.2	0.9
	5	216.6	245.5	239.9	77.9	1.0
	10	232.9	259.2	253.8	74.6	1.1
	20	241.9	275.8	264.5	80.1	0.7
PHB/1 wt% C_{18}MMT	2.5	211.5	238.6	230.0	81.4	1.3
	5	226.3	253.5	246.5	86.6	1.2
	10	245.7	266.4	262.1	69.5	1.3
	20	253.6	284.3	273.7	79.1	1.3
PHB/3 wt% C_{18}MMT	2.5	223.0	248.9	242.0	83.2	2.6
	5	236.7	263.1	256.5	88.3	2.5
	10	254.5	277.8	272.5	75.1	2.9
	20	262.3	293.7	286.0	84.1	2.5
PHB/5 wt% C_{18}MMT	2.5	229.3	251.2	245.3	82.4	3.9
	5	241.4	264.5	259.5	82.2	3.9
	10	260.6	283.1	278.1	77.7	4.2
	20	268.7	295.7	289.1	80.4	3.8
PHB/10 wt% C_{18}MMT	2.5	231.0	245.5	242.8	72.3	7.5
	5	244.1	258.4	256.5	75.3	7.1
	10	262.3	276.1	275.0	61.0	7.8
	20	269.4	287.9	285.5	71.2	7.7

is a simple (one-step) process and can be described by a unique kinetic triplet. This is in agreement with the well-known fact from the literature that thermal degradation of PHB proceeds exclusively by a one step, random chain scission reaction (β-elimination) [35].

Furthermore, based on the results of Fig. 3, it can be assumed that the non-isothermal degradation of PHB/C_{18}MMT nanocomposites proceeds also by a one step process for all relative amounts of the nano-filler, since the values of E estimated are similar to those for PHB and also approximately constant during the whole conversion range. The average values of E in the conversion range between 10–90% and 5–95% are shown in Table 3. Very interesting to note here is that in the PHB/10 wt% C_{18}NMMT the activation energy initially increases to a value larger than that of pure PHB until approximately 15–20% degradation, while afterwards it decreases to values lower than those of pure PHB. This is in agreement with results reported in the previous section, that for this nanocomposite, the degradation started slightly later compared to that with 5 wt% C_{18}NMMT, but it dropped down with a higher rate.

Activation energies were also estimated using the Kissinger method, Eq. (6), and are included in Table 3. The values are in close agreement with the corresponding average values from the KAS method. It seems that in systems, such as those examined here, with a single-step degradation mechanism this simplified method could provide a rough initial estimation of the activation energy.

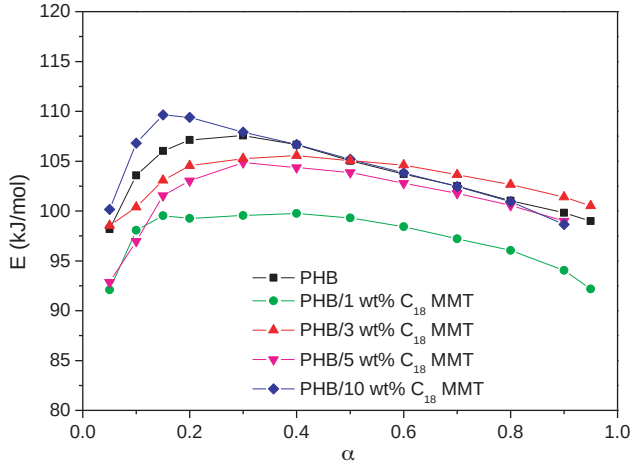

Fig. 3. Variation of the activation energy, E, with α by means of the KAS method for the non-isothermal degradation of PHB and PHB/C_{18}MMT nanocomposites.

4.2. Initial estimation of the kinetic degradation mechanism

A first screening of the kinetic mechanisms can be accomplished by using a simplified version of the Coats–Redfern method. Accordingly, at a specific heating rate, the activation energy can be estimated for every $g(\alpha)$ listed in Table 1 by plotting ($\ln[g(\alpha)/T^2]$) versus $1/T$, according to Eq. (14), which has been successfully applied to other polymer systems [36].

$$\ln\frac{g(\alpha)}{T^2} = \text{Const.} - \frac{E}{RT} \quad (14)$$

Indicative activation energy values for PHB at the conversion interval 5–95% and $\beta = 20$ °C/min, are: 99.1, 63.0, 45.1, 330.9, 356.7, 388.6, 367.2, 161.0, 182.0, 189.9 and 206.9 kJ/mol for the mechanisms A2, A3, A4, D1, D2, D3, D4, R1, R2, R3 and F1, respectively. From these results, it was clear that the F_n, R_n and D_n type models are excluded, since they result in totally different E values or non-linear approximations. Only the A-type mechanism results in E values close to those obtained from the isoconversional models. This initial finding was further investigated using the master plots method proposed by Criado and Malek [29,30]. According to Eqs. (7)–(10) typical plots of $g(\alpha)/g(0.5)$ for PHB appear in Fig. 4. From the results of this figure, it was verified that only the A-type methods describe the experimental data points and these were further investigated.

4.3. Estimation of the invariant kinetic parameters

Furthermore, the IKP method was used for evaluation of the so-called 'true' kinetic triplet i.e. A, E and the expression of $f(\alpha)$. Algebraic expressions for the most frequently used mechanisms are shown in Table 1. Initially the values of $\ln(A)$ and E were estimated using the CR method and only type A and SB models with various n and m values. Indicative values of the estimates of $\ln(A)$ and E for the PHB + 5%C_{18}MMT nanocomposite under different heating rates and n and m combinations are reported in Table 4. Using Eq. (12), the existence of the compensation effect between E and $\ln A$ was checked. Fig. 5 shows the compensation relationship for the non-

Table 3
Average values of E (kJ/mol) obtained by the isoconversional method of KAS at two conversion intervals, as well as by the Kissinger method.

Sample	KAS		Kissinger
	$10\% \le \alpha \le 90\%$	$5\% \le \alpha \le 95\%$	
PHB	104.3 ± 2.6	103.3 ± 3.1	99.4
PHB/1 wt% C_{18}MMT	98.1 ± 1.9	97.1 ± 3.5	100.0
PHB/3 wt% C_{18}MMT	103.6 ± 1.7	102.8 ± 2.8	105.5
PHB/5 wt% C_{18}MMT	101.9 ± 2.5	101.0 ± 3.2	102.1
PHB/10 wt% C_{18}MMT	105.2 ± 3.6	104.7 ± 2.7	104.9

Table 4
Values of E and ln(A) obtained from various kinetic models at various heating rates for PHB + 5% C18MMT nanocomposite (conversion interval 5–90%). R denotes the correlation coefficient of each fitting.

Kinetic Model	5 °C/min			10 °C/min			20 °C/min		
	E (kJ/mol)	ln A	$-R$	E (kJ/mol)	ln A	$-R$	E (kJ/mol)	ln A	$-R$
A0.5	501.3 ± 3.4	112.9 ± 0.79	0.9796	542.5 ± 6.1	118.7 ± 1.35	0.9848	526.0 ± 3.9	113.5 ± 0.86	0.9933
A1	290.8 ± 2.0	65.01 ± 0.47	0.9785	316.0 ± 3.2	68.91 ± 0.71	0.9876	292.6 ± 2.2	63.16 ± 0.47	0.9935
A1.5	220.7 ± 1.6	48.88 ± 0.37	0.9775	240.4 ± 2.2	52.15 ± 0.50	0.9895	214.8 ± 1.6	46.21 ± 0.35	0.9932
A2	185.6 ± 1.3	40.72 ± 0.31	0.9767	202.7 ± 1.8	43.69 ± 0.39	0.9907	175.9 ± 1.4	37.66 ± 0.30	0.9927
A3	150.5 ± 1.1	32.45 ± 0.26	0.9755	164.9 ± ±1.3	35.11 ± 0.29	0.9824	137.0 ± 1.2	28.98 ± 0.25	0.9914
SB0.4–0.3	166.3 ± 0.6	36.61 ± 0.13	0.9948	180.9 ± 0.7	39.16 ± 0.16	0.9980	149.9 ± 0.9	32.28 ± 0.19	0.9957
SB0.6–0.4	138.8 ± 0.6	30.61 ± 0.14	0.9919	151.6 ± 0.5	33.00 ± 0.12	0.9986	120.9 ± 0.7	26.32 ± 0.15	0.9959
SB0.5–0.25	144.8 ± 0.5	31.78 ± 0.10	0.9958	157.7 ± 0.8	34.14 ± 0.18	0.9967	126.0 ± 1.1	27.19 ± 0.23	0.9913
SB0.4–0.4	174.0 ± 0.7	38.43 ± 0.17	0.9924	189.4 ± 0.7	41.09 ± 0.16	0.9983	159.3 ± 0.6	34.39 ± 0.14	0.9981
SB0.5–0.5	164.1 ± 0.8	36.35 ± 0.19	0.9889	179.0 ± 0.8	38.98 ± 0.17	0.9978	149.5 ± 0.6	32.46 ± 0.13	0.9981

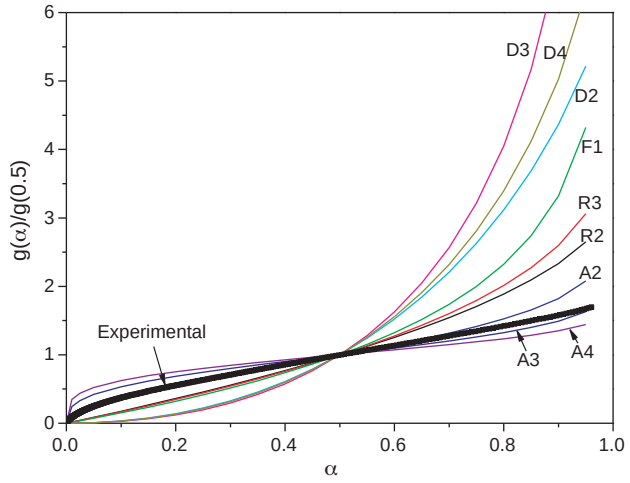

Fig. 4. Theoretical master curves in integral form for the different kinetic models and the experimental data for pure PHB.

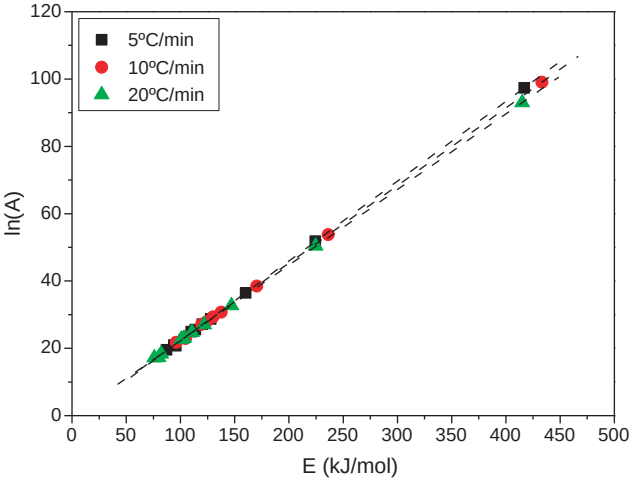

Fig. 5. Typical compensation relationship for PHB.

isothermal degradation of PHB. Similar graphs were obtained for all the PHB/C_{18}MMT nanocomposites.

The slopes and intercepts of these lines give the compensation parameters α^* and b^* at each heating rate. Since the intersection of these lines is dependent on experimental conditions, the calculation of the invariant kinetic parameters is performed using the supercorrelation Eq. (13). Results appear in Fig. 6 and show very good straight lines for all specimens investigated proving, thus, the existence of a supercorrelation relation and permitting the calculation of E_{inv} and A_{inv} from the slope and the intercept, respectively. In the same way, the existence of the compensation effect between E and ln A and the one-step process were confirmed for all nanocomposites. The values of the invariant parameters estimated are illustrated in Table 5. It was noticed that all activation energy values were similar and in the vicinity of 100 kJ/mol. Obtained values of E_{inv} were in very good agreement with corresponding ones estimated by the isoconversional methods and presented in the previous section. Moreover, it should be mentioned here that we did not notice any large fluctuations in the E_{inv} values in contrast

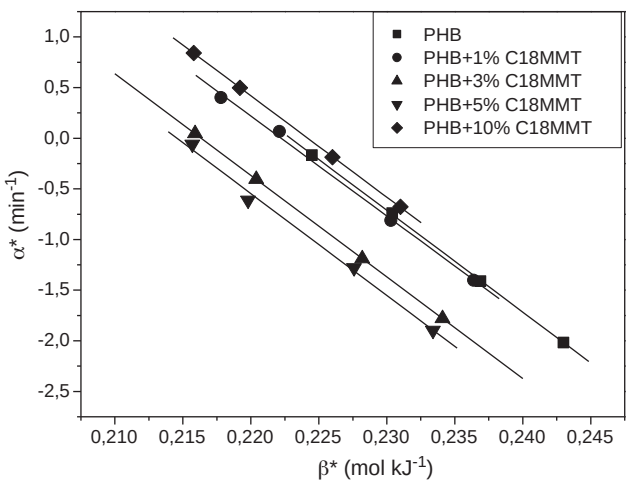

Fig. 6. . Supercorrelation relationship for PHB and all nanocomposites.

Table 5
Values for the invariant kinetic parameters for PHB and all PHB/C_{18}MMT nanocomposites.

Sample	$\ln A_{inv}$ (min^{-1})	E_{inv} (kJ/mol)	R
PHB	22.39 ± 0.41	100.4 ± 1.8	0.9998
PHB/1 wt% C_{18}MMT	21.94 ± 1.15	98.7 ± 5.4	0.9999
PHB/3 wt% C_{18}MMT	21.70 ± 1.50	100.3 ± 7.1	0.9964
PHB/5 wt% C_{18}MMT	21.49 ± 1.74	100.2 ± 6.4	0.9954
PHB/10 wt% C_{18}MMT	22.44 ± 0.34	100.1 ± 1.5	0.9998

to the literature findings, where E_{inv} was found to vary more than 50% (i.e. from 106 to 161 kJ/mol) [15].

4.4. Estimation of the reaction model

According to previous findings, in order to estimate the reaction model that best describes the experimental data only the Avrami–Erofeev and Sestak–Berggren models (Table 1) were investigated here. In order to discriminate betweeen these two models, the criterion proposed by Perez-Maqueda et al. [31] was employed. Accordingly, in a plot of $\ln[(d\alpha/dt)/f(\alpha)]$ versus T^{-1} all experimental data points should lie on a single straight line only when the correct kinetic model is assumed for $f(\alpha)$. The slope and the intercept of this line should give the same values of the activation energy and pre-exponential factor as those initially assumed. Such plots of $\ln[(d\alpha/dt)/f(\alpha)]$ versus T^{-1} for PHB at different heating rates appear in Fig. 7. From the results of this figure, it was clear that only the Sestak–Berggren model resulted in a single straight line. This is in contrast to the results reported by Erceg et al. [15], where it was found that the Avrami–Erofeev model best described the experimental data.

In order to estimate the exponents n and m in the Sestak–Berggren kinetic model $f(\alpha)=\alpha^n(1-\alpha)^m$, it is a common procedure to use linear regression analysis and the assumption that $m/n=(1-\alpha_{max})/\alpha_{max}$ with α_{max} the maximum degree of conversion α. However, when we tried to employ this assumption in this investigation, the results were not satisfactorily. Therefore, we decided to employ a non-linear regression analysis according to the Levenburg–Marquardt method to directly estimate the n and m values at each heating rate without using any linear approximation. The software Origin 8.1 was used. The following procedure was employed: Initially the invariant function, $f_{inv}(\alpha)$ was estimated from Eq. (15), using the invariant parameters A_{inv} and E_{inv} reported in Table 5:

$$f_{inv}(\alpha)=\frac{d\alpha/dt}{A_{inv}\exp(-E_{inv}/RT)} \quad (15)$$

Following, plots of $f_{inv}(\alpha)$ versus α were constructed for each material at all heating rates. Then, the non-linear regression analysis was used by setting $f_{inv}(\alpha)=\alpha^n(1-\alpha)^m$ and estimating the best fit for the n and m parameters. The conversion interval employed was from 5% to 95%. Results together with statistical parameters of the fitting procedure appear in Table 6.

From the results of Table 6 it can be seen that in almost all cases the correlation coefficient, R^2, was very good (i.e. greater than 0.99) and the standard deviation of each value rather low. Furthermore, the dependency of the values was also low (a value close to 1.0 means strong dependency) meaning that the values proposed are independent. Consequently, plots of $\ln[(d\alpha/dt)/f(\alpha)]$ versus T^{-1} were drawn for all nanocomposites and appear in Fig. 8. As it can be seen there, the kinetic model assumed is valid for all nanocomposites, since single straight lines were obtained. From the slopes and the intercept of these straight lines, the 'true' values of E and $\ln A$ can be obtained and are listed in Table 7. These values of activation energy are in very good agreement with the invariant parameters and the values obtained from the isocon-

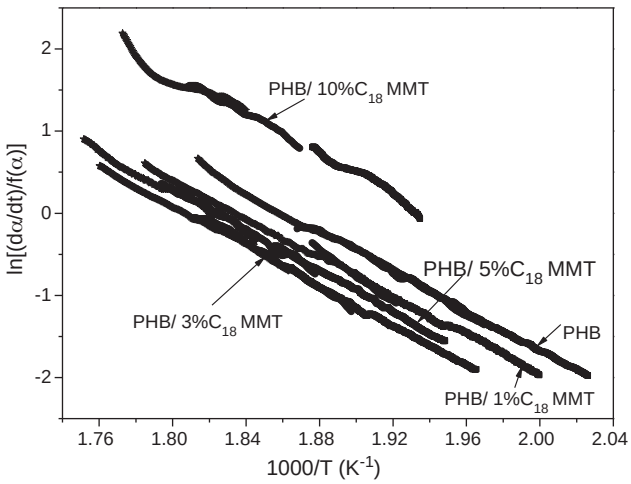

Fig. 8. Plots of $\ln[(d\alpha/dt)/f(\alpha)]$ versus T^{-1} using $f(\alpha)=\alpha^n(1-\alpha)^m$ for pure PHB and all nanocomposites exhibiting very good linearity at all heating rates.

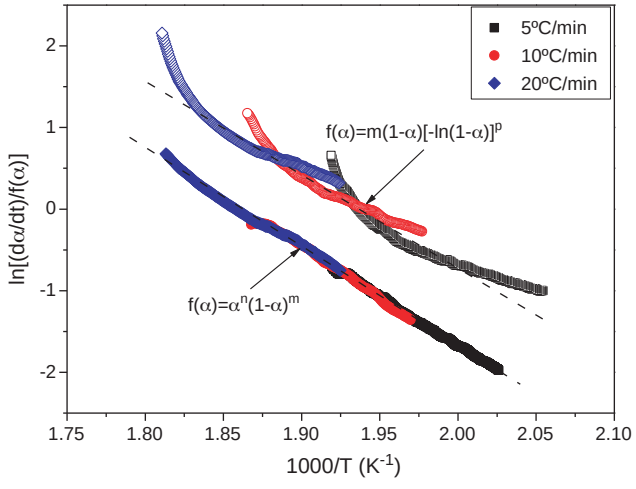

Fig. 7. Plot of $\ln[(d\alpha/dt)/f(\alpha)]$ versus T^{-1} using two kinetic models for $f(\alpha)$, obtained from PHB degradation at various heating rates.

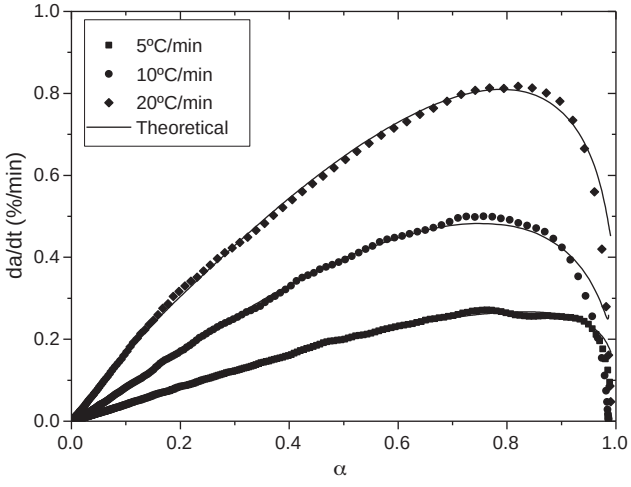

Fig. 9. Comparison of experimental data on the degradation rate versus conversion with the simulation results obtained using the kinetic model $f(\alpha)=\alpha^n(1-\alpha)^m$ for PHB at various heating rates.

Table 6
Best fit values of n and m parameters of the Sestak–Berggren model for pure PHB and all nanocomposites at various heating rates, together with statistical parameters of the non-linear fitting procedure.

Sample	Heating rate (°C/min)	Parameter	Value	Dependency	χ^2/Dof	R^2
PHB	5	*n*	0.515 ± 0.002	0.094	0.0001	0.9963
		m	0.262 ± 0.001	0.105		
	10	*n*	0.482 ± 0.002	0.095	0.0002	0.9940
		m	0.262 ± 0.002	0.098		
	20	*n*	0.432 ± 0.004	0.094	0.0001	0.9906
		m	0.382 ± 0.003	0.098		
PHB/1 wt% C_{18}MMT	5	*n*	0.542 ± 0.002	0.098	0.0001	0.9945
		m	0.202 ± 0.002	0.098		
	10	*n*	0.514 ± 0.009	0.104	0.0037	0.9876
		m	0.378 ± 0.012	0.104		
	20	*n*	0.485 ± 0.001	0.107	0.0001	0.9952
		m	0.357 ± 0.001	0.107		
PHB/3 wt% C_{18}MMT	5	*n*	0.623 ± 0.001	0.098	0.0001	0.9973
		m	0.167 ± 0.001	0.098		
	10	*n*	0.621 ± 0.005	0.099	0.0013	0.9649
		m	0.235 ± 0.005	0.099		
	20	*n*	0.555 ± 0.001	0.099	0.0001	0.9976
		m	0.253 ± 0.001	0.099		
PHB/5 wt% C_{18}MMT	5	*n*	0.795 ± 0.001	0.108	0.0001	0.9978
		m	0.276 ± 0.001	0.108		
	10	*n*	0.836 ± 0.003	0.125	0.0004	0.9922
		m	0.422 ± 0.003	0.125		
	20	*n*	0.673 ± 0.003	0.165	0.0005	0.9687
		m	0.434 ± 0.003	0.165		
PHB/10 wt% C_{18}MMT	5	*n*	1.449 ± 0.002	0.181	0.0001	0.9965
		m	0.667 ± 0.001	0.181		
	10	*n*	1.385 ± 0.005	0.191	0.0001	0.9934
		m	0.832 ± 0.004	0.191		
	20	*n*	1.221 ± 0.004	0.170	0.0001	0.9928
		m	0.734 ± 0.003	0.170		

Table 7
'True' values of *E* and ln *A* and average values of the *n* and *m* parameters for pure PHB and all nanocomposites.

Sample	$\ln(A_{true})$ (min^{-1})	E_{true} (kJ/mol)	R^2	n_{aver}	m_{aver}
PHB	22.36	100.3	0.9993	0.48	0.30
PHB/1 wt% C_{18}MMT	21.55	97.7	0.9996	0.51	0.31
PHB/3 wt% C_{18}MMT	22.08	101.5	0.9993	0.60	0.22
PHB/5 wt% C_{18}MMT	22.41	102.2	0.9992	0.77	0.38
PHB/10 wt% C_{18}MMT	24.02	103.3	0.9995	1.35	0.74

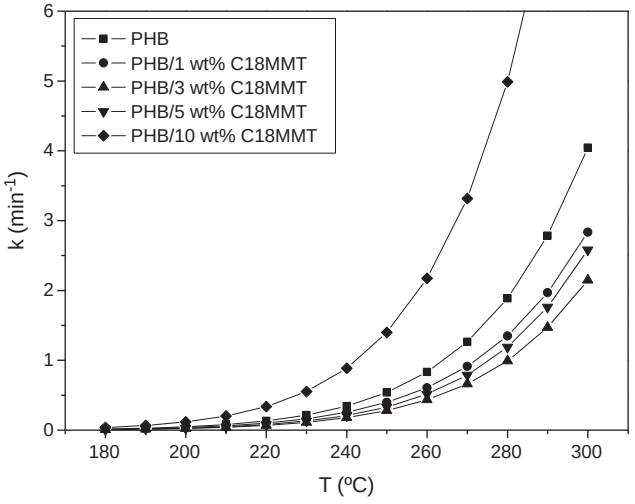

Fig. 10. Dependence of *k* on *T* for pure PHB and PHB nanocomposites.

versional analysis. The average values of the *n* and *m* parameters appear also in Table 7. For PHB, the average values of *n* and *m* estimated (i.e. 0.5 and 0.3, respectively) are in very good agreement to corresponding values obtained from isothermal degradation experiments (i.e. 0.6 and 0.3, respectively) [18]. Furthermore, an increase of *n* with the amount of the nanofiller was observed, while the effect on *m* was not so clear; the values of *m* initially decrease until 3 wt% C_{18}MMT, while afterwards they tend to increase. If we keep in mind that the *n* exponent denotes an acceleratory reaction, while *m* a decay region of thermal degradation, then the tendency of the estimated values is that the increase in the amount of the nano-filler increases the acceleratory mechanism, while it initially decreases but afterwards increases the decay reaction. Finally, since always the values of *n* are larger than the corresponding of *m*, it is an indication that the accelerator reaction of thermal degradation of PHB and of all nanocomposites is always larger than the decay reaction.

To check the accuracy of the proposed model that describes the experimental data, the values of $d\alpha/dt$ obtained experimentally were compared to corresponding ones from the simulation model results. An indicative plot is illustrated in

Fig. 9. A very good agreement between the experimental data and the simulation results was observed at all heating rates employed.

Finally, the 'true' values of E and $\ln A$ allow us to calculate the rate constant, k, of the non-isothermal degradation of pure PHB and of all nanocomposites. Data are presented in Fig. 10. The addition of C_{18}MMT reduces the rate constant compared to pure PHB, i.e. the rate of the non-isothermal degradation of PHB. This is probably due to the fact that layered silicates act as mass transport barriers into and out of the degradation zone. Accordingly, thermal decomposition begins from the surface of the nanocomposites, leading in an increase of the organo-MMT content and the formation of a "protection layer" by the clay. This so-called "barrier model" may work well for char-forming polymers, but it seems to not hold for non-char-forming polymers [37,38]. According to Vyazovkin et al. [37,38] nanoconfinement appears to present a more specific description of the phenomenon. According to this theory, polymer degradation starts and the newly formed radicals are nanoconfined, permitting a variety of bimolecular reactions to occur. As degradation progresses, the clay platelets, driven by a decrease in the surface free energy, migrate gradually to the surface and form the barrier that has been also detected experimentally.

5. Conclusions

Study of the thermal degradation kinetics of nanocomposites based on PHB and organo-modified clays reveals that the thermal stability of the material is improved by the addition of the nano-filler. From an isoconversional analysis using the FWO and KAS methods, it was found that the activation energy does not vary significantly with the degree of degradation denoting degradation in one step with similar values for pure PHB and for all nanocomposites.

Furthermore, using the invariant kinetic parameters method, the particular reaction model and the so-called 'true' values of the activation energy and pre-exponential factor, A, were determined. It was found that the model that best describes the experimental data was that of Sestak–Berggren with $f(a) = \alpha^n(1-\alpha)^m$. The value of the 'true' activation energy was found to be about 100 kJ mol^{-1} for all nanocomposites and the pre-exponential factor for PHB was estimated equal to 5.35×10^9 min^{-1}. Finally, the values of the kinetic rate constant k were found to decrease with the amount of the nano-filler up to 3 wt%, while for amounts larger than 3 wt% k increased reaching a value greater than that of pure PHB for the 10 wt% nanocomposites.

References

[1] E.G. Fernandes, M. Pietrini, E. Chiellini, Thermo-mechanical and morphological characterization of plasticized poly [(R)-3-hydroxybutyric acid], Macrom. Symp. 218 (2004) 157–164.
[2] S.N. Lee, M.Y. Lee, W.H. Park, Thermal stabilization of poly(3-hydroxybutyrate) by poly(glycidyl methacrylate), J. Appl. Polym. Sci. 83 (2002) 2945–2952.
[3] P. Bordes, E. Pollet, L. Averous, Nano-biocomposites: biodegradable polyester/nanoclay systems, Prog. Polym. Sci. 34 (2009) 125–155.
[4] D.S. Achilias, M.M. Karabela, I.D. Sideridou, Thermal degradation of light-cured dimethacrylate resins Part I. Isoconversional kinetic analysis, Thermochim. Acta 472 (2008) 74–83.
[5] D.S. Achilias, M.M. Karabela, I.D. Sideridou, Thermal degradation and isoconversional kinetic analysis of light-cured dimethacrylate copolymers, J. Therm. Anal. Calorim. 99 (2010) 917–923.
[6] S. Vyazovkin, N. Sbirrazzuoli, Isoconversional kinetic analysis of thermally stimulated processes in polymers, Macromol. Rapid Commun. 27 (2006) 1515–1532.
[7] C. Chen, B. Fei, S. Peng, Y. Zhuang, L. Dong, Z. Feng, The kinetics of the thermal decomposition of poly(3-hydroxybutyrate) and maleated poly(3-hydroxybutyrate), J. Appl. Polym. Sci. 84 (2002) 1789–1796.
[8] M.Y. Lee, T.S. Lee, W.H. Park, Effect of side chains on the thermal degradation of poly(3-hydroxybutyrate), Macromol. Chem. Phys. 202 (2001) 1257–1261.
[9] S.D. Li, J.D. He, P.H. Yu, M.K. Cheung, Thermal degradation of poly(3-hydroxybutyrate) and poly(3-hydroxybutyrate-co-3-hysroxyvalerate) as studied by TG TG-FTIR and Py-GC/MS, J. Appl. Polym. Sci. 89 (2003) 1530–1536.
[10] A.F. Santos, L. Polese, M.S. Crespi, C.A. Ribeiro, Kinetic model of poly(3-hydroxybutyrate) thermal degradation from experimental non-isothermal data, J. Therm. Anal. Calorim. 96 (2009) 287–291.
[11] H. Ariffin, H. Nishida, Y. Shirai, M.H. Hassan, Determination of multiple thermal degradation mechanisms of poly(3-hydroxybutyrate), Polym. Degrad. Stabil. 93 (2008) 1433–1439.
[12] M. Kawalec, H. Janeczek, G. Adamus, P. Kurcok, M. Kowalczuk, M. Scandola, The study of kinetics of poly[(R,S)-3-hydroxybutyrate] degradation induced by carboxylate, Macromol. Symp. 272 (2008) 63–69.
[13] E. Hablot, P. Bordes, E. Pollet, L. Averous, Thermal and thermo-mechanical degradation of poly(3-hydroxybutyrate)-based multiphase systems, Polym. Degrad. Stab. 93 (2008) 413–421.
[14] P. Bordes, E. Hablot, E. Pollet, L. Averous, Effect of clay organomodifiers on degradation of polyhydroxyalkanoates, Polym. Degrad. Stab. 94 (2009) 789–796.
[15] M. Erceg, T. Kovacic, S. Perinovic, Kinetic analysis of the non-isothermal degradation of poly(3-hydroxybutyrate) nanocomposites, Thermochim. Acta 476 (2008) 44–50.
[16] M. Erceg, T. Kovacic, I. Klaric, Thermal degradation and kinetic analysis of poly(3-hydroxybutyrate)/organoclay nanocomposites, Macromol. Symp. 267 (2008) 57–62.
[17] M. Erceg, T. Kovacic, I. Klaric, Poly(3-hydroxybutyrate) nanocomposites: isothermal degradation and kinetic analysis, Thermochim. Acta 485 (2009) 26–32.
[18] T.M. Wu, S.F. Hsu, Y.F. Shih, C.S. Liao, Thermal degradation kinetics of biodegradable poly(3-hydroxybutyrate)/layered double hydroxide nanocomposites, J. Polym. Sci.: Part B: Polym. Phys. 46 (2008) 1207–1213.
[19] S.I. Marras, A. Tsimpliaraki, I. Zuburtikudis, C. Panayiotou, Thermal and colloidal behavior of amine-treated clays: the role of amphiphilic organic cation concentration, J. Colloid Interf. Sci. 315 (2007) 520.
[20] J.D. Peterson, S. Vyazovkin, C.A. Wight, Kinetics of the thermal and thermo-oxidative degradation of polystyrene, polyethylene and polypropylene, Macromol. Chem. Phys. 202 (2001) 775–784.
[21] H.L. Friedman, Kinetics of thermal degradation of char-forming plastics from thermogravimetry. Application to phenolic plastic, J. Polym. Sci. C: Polym. Symp 6PC (1964) 183–195.
[22] C.D. Doyle, Kinetic analysis of thermogravimetric data, J. Appl. Polym. Sci. 5 (1961) 285–292.
[23] J.H. Flynn, L.A. Wall, General treatment of the thermogravimetry of polymers, J. Res. Natl. Bur. Stand. 70A (1966) 487–523.
[24] T. Ozawa, A new method of analyzing Thermogravimetric data, Bull. Chem. Soc. Jpn. 38 (1965) 1881–1886.
[25] S. Vyazovkin, Modification of the integral isoconversional method to account for variation in the activation energy, J. Comput. Chem. 22 (2001) 178–183.
[26] S. Vyazovkin, Evaluation of activation energy of thermally stimulated solid state reactions under arbitrary variation of temperature, J. Comput. Chem. 18 (1997) 393–402.
[27] H.E. Kissinger, Anal. Chem. 29 (1957) 1702.
[28] P. Budrugeac, E. Segal, Applicability of the Kissinger equation in thermal analysis, Revisited, J. Therm. Anal. Calorim. 88 (2007) 703–707.
[29] F.J. Gotor, J.M. Criado, J. Malek, N. Koga, Kinetic analysis of solid-state reactions: the universality of master plots for analyzing isothermal and nonisothermal experiments, J. Phys. Chem. A 104 (46) (2000) 10777–10782.
[30] J.M. Criado, J. Malek, A. Ortega, Applicability of the master plots in kinetic analysis of non-isothermal data, Thermochim. Acta 147 (1989) 377–385.
[31] L.A. Perez-Maqueda, J.M. Criado, F.J. Gotor, J. Malek, Advantages of combined kinetic analysis of experimental data obtained under any heating profile, J. Phys. Chem. A 106 (12) (2002) 2862–2868.
[32] P. Budrugeac, E. Segal, L.A. Perez-Maqueda, J.M. Criado, The use of the IKP method for evaluating the kinetic parameters and the conversion function of the thermal dehydrochlorination of PVC from non-isothermal data, Polym. Degrad. Stabil. 84 (2004) 311–320.
[33] A.W. Coats, J.P. Redfern, Nature 201 (1964) 68.
[34] A.I. Lesnikovich, S.V. Levchik, A method of finding invariant values of kinetic-parameters, J. Therm. Anal. 27 (1983) 89–94.
[35] F.D. Kopinke, K. Mackenzie, Mechanistic aspects of the thermal degradation of poly(lactic acid) and poly(β-hydroxybutyric acid), J. Anal. Appl. Pyrol. 40–41 (1997) 43–53.
[36] L. Nunez, F. Fraga, M.R. Nunez, M. Villanueva, Thermogravimetric study of the decomposition process of the system BADGE ($n = 0$)/1, 2 DCH, Polymer 41 (2000) 4635–4641.
[37] K. Chen, C.A. Wilkie, S. Vyazovkin, Nanoconfinement revealed in degradation and relaxation studies of two structurally different polystyrene–clay systems, J. Phys. Chem. B 111 (2007) 12685–12692.
[38] K. Chen, K. Harris, S. Vyazovkin, Tacticity as a factor contributing to the thermal stability of polystyrene, Macromol. Chem. Phys. 208 (2007) 2525–2532.